# Microcosm assessment of the biogeochemical development of sulfur and oxygen in oil sands fluid fine tailings

Michael Chen [a], Gillian Walshe [a], Ernest Chi Fru [a,c], Jan J.H. Ciborowski [b], Christopher G. Weisener [a,*]

[a] Great Lakes Institute for Environmental Research, University of Windsor, Windsor, Ontario N9B 3P4, Canada
[b] Department of Biological Sciences, University of Windsor, Windsor, Ontario N9B 3P4, Canada
[c] Swedish Museum of Natural History, Nordic Centre for Earth Evolution, Department of Paleobiology, P.O. Box 50007, SE-104 05 Stockholm, Sweden

## ARTICLE INFO

## ABSTRACT

Bitumen recovery from Alberta oil sands generates fluid fine tailings, which are retained in tailings ponds where solids settle and release process water. The recovered water is recycled for bitumen extraction, while the resulting tailings are incorporated into various landforms for reclamation, with one option being conversion of tailings basins to viable end pit lakes. Tailings ponds commonly host diverse microbial communities, including $SO_4$-reducing prokaryotes. The highly reducing nature of the hydrogen sulfide produced by these prokaryotes may impact the biogeochemical cycling of key nutrients. However, the behavioral dynamics of hydrogen sulfide production in ponds containing fluid fine tailings remain to be clearly explained. In this study, microcosms are used as analogues of the sediment–water interface of a tailings pond undergoing reclamation to determine sulfide generation patterns and the behavior of $O_2$. In the microcosms, hydrogen sulfide fluxes correlated positively with biotic activity, reaching levels of over $2 \times 10^3$ nmol cm$^{-2}$ s$^{-1}$, leading to Fe sulfide formation. Depth-related hydrogen sulfide profiles in the microcosms were comparable to those encountered in situ, in Syncrude's West In-Pit, an active tailing pond. Oxygen diffusion across the fluid fine tailing sediment–water interface was controlled to different degrees by both biotic and abiotic processes. The results have implications for quantitatively estimating the impact of hydrogen sulfide production, $O_2$ availability, and biogeochemical cycling of key nutrients important for the success of life in fluid fine tailings-affected ecosystems. This paper shows that this production of hydrogen sulfide may be a self-limiting process, which will begin to decrease after a period of time.

© 2013 Elsevier Ltd. All rights reserved.

## 1. Introduction

The Athabasca oil sands in northeastern Alberta, Canada comprise the third largest hydrocarbon reserve in the world next to Saudi Arabia and Venezuela, estimated at ~1.7 trillion barrels of recoverable bitumen (Chalaturnyk et al., 2002; Alberta Energy, 2013). Currently, ~1.3 million barrels are extracted daily for commercial use (Alberta Energy and Utilities Board, 2007; Alberta Energy, 2013), and production is anticipated to grow following new advances in extraction technologies, coupled with global decline of conventional oil reservoirs (Williams, 2003). With new projects added annually, production is expected to reach 3 million barrels/day by 2018 (Alberta Energy, 2013).

After surface mining, bitumen is separated from the oil sands ore by a warm water process, resulting in tailings consisting of 20–30 wt% solids (mostly clay and sand), ~3 wt% residual bitumen, and alkaline water (Chalaturnyk et al., 2002). Producers comply with a zero-discharge policy, by transferring tailings to on-site

tailings ponds, where the sand quickly settles out and the resulting clay suspension is allowed to dewater through density-dependent settling, which produces fluid fine tailings (FFT). The released water is either recycled for further bitumen extraction or discharged and used for on-site landscape reconstruction (Siddique et al., 2006). The consolidated FFT is destined for integration into reclaimed landforms, and one option being considered is conversion of existing tailings ponds into future end-pit lakes (EPLs). The tailings pond water cap has a unique chemical composition, consisting mostly of recycled process water containing elevated $Na^+$ (termed brackish) concentrations, $SO_4^{2-}$ and $Cl^-$ anions, naphthenic acids and $NH_3$. Current evidence suggests natural attenuation mechanisms result in the removal or degradation of naphthenic acid compounds and $NH_3$, as well as a general shift in the water chemistry toward less saline natural water composition as the system ages (Scott et al., 2005). The underlying chemical factors contributing to the processes operating during maturation between the FFT sediment and overlying water in tailing pond basins, however, still require explanation.

In order to develop a sustainable aquatic ecosystem in locations such as reclaimed EPLs, it is essential to have a detailed

---

* Corresponding author. Tel.: +1 519 253 3000x3753; fax: +1 519 971 3616.
E-mail address: weisener@uwindsor.ca (C.G. Weisener).

understanding of the long term impacts that FFT will have on both the physical environment and living organisms as these systems develop. This study addresses these issues by focusing on the biotic and abiotic processes contributing to the development of key elemental cycles (e.g. S, Fe, N, and C) that may perturb or stabilize these reclaimed environments. Assessing the short and long term biogeochemical drivers, as well as production rates of highly reactive dissolved species, like $HS^-$, will be essential to predicting the establishment of these elemental cycles. Faunal abundance and biomass in natural aquatic ecosystems correlate positively with sediment $O_2$ demand (SOD) (Tahey et al., 1994), which is comprised of biological $O_2$ demand (BOD) and chemical $O_2$ demand (COD) (Wang and Reed, 1984; Gelda et al., 1995). COD dominates epibenthic processes found in young marshes created with oil sands process material (OSPM) (Gardner Costa, 2010).

In this context, the SOD function of the FFT will directly influence dissolved $O_2$ (DO) concentrations in the water column, and thus, can be affected by a combination of biological (i.e., bacteria – BOD) and chemical processes (COD) occurring at the FFT sediment–water interface. The principal source of BOD is the biological respiration associated with bacterial decay processes at the FFT sediment–water interface. This biological activity can influence the release of chemically reduced compounds via bacterial respiration, such as iron, sulfide, methane and ammonia. These soluble compounds will exert a rapid kinetic $O_2$ demand as the reduced materials undergo oxidation (Gelda et al., 1995; Matzinger et al., 2010).

Current data suggest various microbial consortia responsible for driving distinct redox-dependent biogeochemical processes have developed in established FFT settling basins (Penner and Foght, 2010; Ramos-Padrón et al., 2011). These complex associations include anaerobic heterotrophs, sulfate-reducing prokaryotes (SRP), and methanogens (Clemente and Fedorak, 2005; Siddique et al., 2006, 2007; Penner and Foght, 2010; Ramos-Padrón et al., 2011). Substantial evidence also indicates that S cycling will be crucial in governing successional processes in EPL settings, and seems to be a dominant determinant of the spatial organization of the various microbial communities (Penner and Foght, 2010; Ramos-Padrón et al., 2011; Chi Fru et al., 2013) linked to sulfide production and methanogenesis (Holowenko et al., 2000; Salloum et al., 2002).

However, little is known about the specific rates of generation and consumption of key oxidants and reductants in EPLs, such as $O_2$, $SO_4^{2-}$ and $HS^-$ or the factors responsible for controlling the biogeochemical dynamics of these redox-sensitive species. This is especially true for $HS^-$ generation, as this can stress eukaryotic organisms (Williford et al., 2009). The $HS^-$ production might critically limit microbial and metazoan colonization in the overlying water column, where natural communities are expected to develop following the reclamation of the previously mined areas. In addition, $HS^-$ plays a key role in regulating trace metal solubility in many aquatic environments, especially Fe, which precipitates to form Fe sulfides (Schoonen, 2004). Iron is important both as an essential trace element for microbial growth (Archer and Johnson, 2000; Church et al., 2000), and as a terminal electron acceptor and donor during microbial metabolism (Weber et al., 2006; Crowe et al., 2007; Chi Fru et al., 2012). Thus, $HS^-$ generation linked to SRP individuals within EPLs may play a fundamental role in both Fe cycling and microbial growth.

As mentioned above, $O_2$ availability will be a factor determining the speed and success of microbial colonization and sustainability in EPLs, especially in laying the foundation for establishing aquatic conditions that can sustain a complete food web. In addition, rates of $O_2$ diffusion into the FFT will determine the degradation rates of recalcitrant hydrocarbons. Hydrocarbons are much more biodegradable under oxic conditions (Leahy and Colwell, 1990).

However, specific groups of microorganisms, such as some members of the SRP can degrade hydrocarbons under anoxic conditions (Rueter et al., 1994). In particular, naphtha (a residual solvent remaining in the FFT after froth treatment) and organic acids present in the original oil sands ore that are concentrated during the extraction process can be biodegraded both in the absence and presence of $O_2$ (Scott et al., 2005; Siddique et al., 2006, 2007, 2011). Therefore, the development of redox gradients in the FFT, as a function of $O_2$ availability and demand, will likely facilitate various biogeochemical processes at different rates.

This study investigates the behavior of S and $O_2$ at the FFT–oil sand process water (OSPW) interface, in order to assess these primary chemical components in EPL settings over short and long term time periods, using a combination of microcosms. Previous work (Chi Fru et al., 2013) demonstrated the ability of this approach to faithfully simulate *in situ* development of microbial community structures similar to those observed in the existing West In-Pit lake (WIP) storage basin. This study compares the development of a defined redox front in both field and laboratory settings for the WIP material, which may influence the geochemical cycling of elements within the pond. Specifically, the experiment poses and answers the question of whether these processes are predominantly regulated by biotic or abiotic driven activity, with respect to S and $O_2$.

## 2. Materials and methods

### 2.1. Microcosm setup

Approximately 200 L of fresh FFT and 150 L of OSPW samples were collected from the West In-Pit (WIP) tailings pond operated by Syncrude Canada Ltd., approximately 40 km north of Fort McMurray. The tailings pond is part of the In-pit facility (formerly mined out area) that was commissioned in 1995. The tailings pond was isolated from the tailings process system in 2012 and is being considered for reclamation as an end pit lake containing water-capped FFT as part of Syncrude's reclamation strategy. The FFT sample consists of 33 wt% solids (e.g., sand, clay, etc.), 65 wt% water with residual 1.97 wt% bitumen (Table 1), and less than 0.06 wt% soluble organics (not shown). The samples were collected 10 M below the mudline and are considered to be FFT based on water content. Samples collected were stored and shipped at 4 °C. A subset of FFT samples (100 L) and OSPW (75 L) was gamma irradiated at 28 kGy for 24 h, at the McMaster Institute of Applied Radiation Services (McIARS), Hamilton, Ontario, Canada to serve as a sterile control.

A $2 \times 2$ factorial study design was used to distinguish the effects of atmosphere (oxic vs. anoxic environments) and microbial activity (biotic vs. abiotic microcosms) on the evolution of S and $O_2$ ($n = 10$ replicate microcosms per treatment). Microcosms were constructed from ethanol-sterilized 4 L Camwear® containers purchased from Cambro Manufacturing Company. The anoxic microcosms were fitted with covers equipped with O-ring airtight seals and two push-plug valves for headspace gas sampling and purging, if required (Fig. 1).

The FFT was thoroughly mixed using a power portable drill to which was attached a sterilized Teflon-coated stirring paddle. A 2000-g aliquot of FFT was added to each microcosm and overlaid with 1000 mL of OSPW. Anoxic microcosms were then flush cycled with ultra pure $N_2$ gas for 5 min, and cycled additionally when set inside the gas (95% $N_2$, 5% $H_2$ mixture) chamber. Oxic microcosms were incubated on shelves with unmodified lids without seals. All microcosms were kept in darkness at 22 °C. Individual microcosms were destructively analyzed after 0, 6, 24, 36, and 52 weeks ($n = 2$ per treatment).

**Table 1**
Description of bulk FFT material and chemical characterization of FFT and OSPW from Syncrude research laboratories before (biotic) and after (abiotic) gamma irradiation.

| | Bulk FFT | Biotic FFT | Abiotic FFT | Biotic OSPW | Abiotic OSPW |
|---|---|---|---|---|---|
| Solids (%)[a] | 33.37 | | | | |
| Water (%)[a] | 64.65 | | | | |
| Bitumen (%)[a] | 1.98 | | | | |
| pH | | 7.82 | 8.19 | 7.96 | 8.31 |
| Conductivity ($\mu$S/cm) | | 3550 | 3200 | 3320 | 3300 |
| Naphtha (% by wt) | | 0.05 | 0.05 | NA | NA |
| *Anions* (ppm) | | | | | |
| $CO_3^{2-}$ | | 123 | 137 | 15 | 12.3 |
| $HCO_3^-$ | | 1250 | 1190 | 574 | 639 |
| $F^-$ | | BDL | BDL | BDL | BDL |
| $Cl^-$ | | 570 | 580 | 510 | 510 |
| $NO_2^-$ | | BDL | BDL | BDL | BDL |
| $NO_3^-$ | | BDL | BDL | 68 | BDL |
| $PO_4^-$ | | BDL | BDL | BDL | BDL |
| $SO_4^-$ | | 3.37 | 12.2 | 518 | 528 |
| $Br^-$ | | BDL | BDL | BDL | BDL |
| *Cations* (ppm) | | | | | |
| $Na^+$ | | 863 | 866 | 796 | 761 |
| $K^+$ | | 16.6 | 17.9 | 16.6 | 16.2 |
| $Mg^{2+}$ | | 12.3 | 11.7 | 13.4 | 13.0 |
| $Ca^{2+}$ | | 21.7 | 20.2 | 24.2 | 23.2 |
| $NH_4^+$ | | 10.4 | 13.4 | BDL | 4.0 |
| *Trace metals* (ppm) | | | | | |
| Al | | 0.092 | 0.660 | 0.178 | 1.240 |
| Sb | | BDL | BDL | BDL | BDL |
| Ba | | 0.529 | 0.484 | 0.218 | 0.192 |
| B | | 4.19 | 3.47 | 2.54 | 2.45 |
| Cd | | BDL | BDL | BDL | BDL |
| Ca | | 21.7 | 20.2 | 24.2 | 23.2 |
| Cr | | BDL | BDL | BDL | BDL |
| Co | | BDL | BDL | BDL | BDL |
| Cu | | BDL | BDL | BDL | BDL |
| Fe | | BDL | 0.172 | 0.020 | 0.396 |
| Pb | | BDL | BDL | BDL | BDL |
| Li | | BDL | BDL | BDL | BDL |
| Mg | | 12.3 | 11.7 | 13.4 | 13.0 |
| Mn | | 0.073 | 0.049 | 0.058 | 0.083 |
| Mo | | BDL | BDL | 0.15 | 0.15 |
| Ni | | BDL | BDL | BDL | BDL |
| P | | BDL | BDL | BDL | BDL |
| K | | 16.6 | 17.9 | 16.6 | 16.2 |
| Se | | BDL | BDL | BDL | BDL |
| Si | | 6.25 | 5.79 | 2.45 | 3.99 |
| Na | | 863 | 866 | 796 | 761 |
| Sr | | 0.794 | 0.745 | 0.825 | 0.800 |
| S | | 5.12 | 7.00 | 185.00 | 177.00 |
| Ti | | 0.027 | 0.037 | 0.028 | 0.055 |
| V | | 0.031 | 0.036 | 0.035 | 0.035 |
| Zn | | BDL | BDL | BDL | BDL |
| Zr | | BDL | BDL | BDL | BDL |

NA: not analyzed.
BDL: below detection limit; all values are expressed as ppm.
  [a] Bulk FFT material analysis was done by Syncrude.

## 2.2. In situ electrochemical measurements

Practical applications of these sensors on environmental samples have been investigated by Revsbech (1989), Elberling and Damgaard (2001), Arega and Lee (2005), and Sørensen et al. (2009). Micromanipulator-mounted, micro-electrode sensors were purchased from Unisense Science (Denmark). These are characterized by their linear response to specific media, providing accurate micrometer scale measurements (Damgaard et al., 1995). Microsensors with tip diameters between 100 and 500 $\mu$m were calibrated before each experimental period. The individual sensors were used to monitor changes in pH, Eh, $O_2$ and $HS^-$ at multiple water and FFT depths across the FFT–OSPW interface within the microcosms.

## 2.3. Diffusivity measurements

Diffusivity measurements of the FFT were obtained using a 50-$\mu$m diameter tip Unisense diffusivity sensor which uses an amperometric sensor equipped with a micro-transducer surrounded by a tracer ($H_2$) gas reservoir with a tip membrane. The signal of the microsensor was calibrated to provide diffusivity coefficients at the FFT–OSPW interface using a two-point calibration after Revsbech et al. (1998). The microsensor data collection and interpretation assumes that the microcosms are one-dimensional systems, (i.e., the environment in the two horizontal dimensions is relatively homogeneous) so that a depth profile can be applied for calculating fluxes. The concentration at any given depth in a microcosm was obtained through the undifferentiated concentration profile from
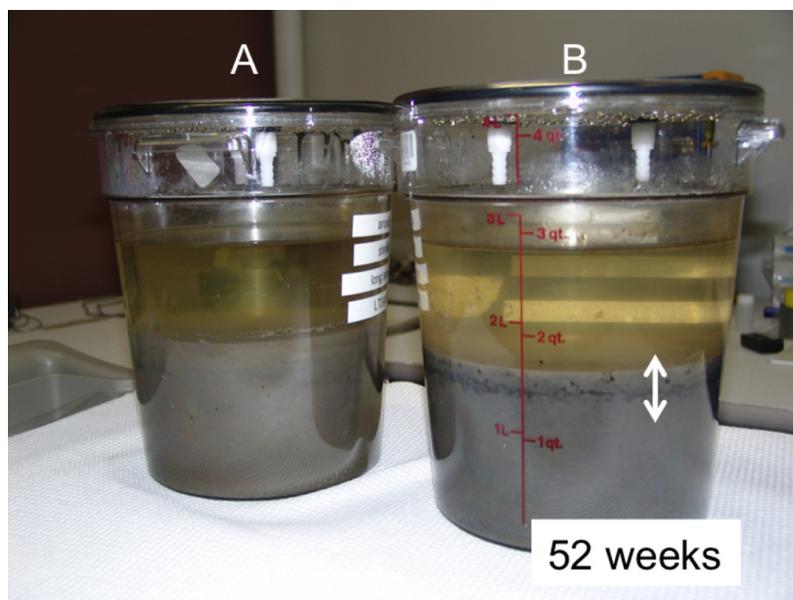
**Fig. 1.** Two sealed anoxic microcosms after 52 weeks (A) represents the sterilized abiotic system and (B) represents the biotic system. The double arrow denotes the black zonation formed by sulfide within this system.

$O_2$ and $HS^-$ sensors. Then using Fick's first law of diffusion, the flux of $HS^-$ or $O_2$ molecules was calculated as follows:

$$J(x) = -\phi D(x)\frac{dC(x)}{dx} \qquad (1)$$

$J$ is the diffusion flux (amount of substance per unit area per unit time); the amount of substance that will flow through a small area during a small time interval. $D$ represents the diffusion coefficient or diffusivity in dimensions of space and time, the diffusivity microsensor measures this as ($cm^2/s$). $\phi$ stands for the concentration in dimensions of amount of substance multiplied by the length. The flux describes the vertical transport of the substance through the specific layer, and can summarize the exchange of the substance across the FFT–OSPW interface. The first derivative of the concentration profile, (the slope) represents the vertical transport of the molecules between specific points along the depth profile, indicating the exchange of molecules at the boundary defined by the FFT–OSPW interface. Hofman et al. (1991) and Glud (2008) had specifically applied Fick's Law in benthic oxygen availability of marine systems. The FFT and OSPW that have been processed through extraction and purification of oil sands ore are relatively homogenous when compared to native aquatic sediments and water, therefore, it is reasonable to apply Fick's Law to this particular study.

### 2.4. Spectroscopic characterization

The composition of particulate materials in the original FFT was compared with samples collected after 6 and 36 weeks from the biotic microcosms, and examined using a FEI Quanta 200F environmental scanning electron microscope (ESEM) under low vacuum at 15 kV. Both backscattered electron (BSE) and secondary electron (SE) detectors were used. Energy dispersive spectroscopy (EDS) analysis was performed to confirm the elemental composition of minerals with time. The Genesis Particle Phase cluster analysis software was used for modal mineralogical determinations based on 4000 individual particles. The modal percentages are calculated on the proportion of sulfides relative to accessory minerals within the matrix material (Weisener and Weber, 2010). In addition, X-ray diffraction (XRD) patterns of representative samples of FFT were studied at the National Research Council (NRC) in Ottawa, Ontario,

Canada using a RIGAKU D/MAX 2500 rotating-anode powder diffractometer, with monochromatic Cu K$\alpha$ radiation at 50 kV, 260 mA, a step-scan 0.02°, at a scan rate of 1°/min in 2$\theta$ from 5° to 70°.

### 2.5. Field analysis

FFT field samples were collected from Syncrude Canada Ltd.'s WIP settling basin, in September 2011 (UTM coordinates N 6318795, E 463036) using a piston drive sampler. The piston is released, drawing FFT into the sampler. Sampling started at the FFT–OSPW interface at 0.5-m intervals to a depth of 10 m, after which the samples were taken every 5 m to a depth of 25 m, providing optimum vertical scale resolution. The FFT was processed under anoxic conditions at site and sealed in glass jars with no headspace. Samples were divided into subsets on the drill platform for later chemical and physical characterization using standard operating procedures (Syncrude Canada Ltd., 1995) for porewater characterization, particle size analysis and general geochemical parameter determinations. Additional samples were collected for future molecular and trace metal/mineralogical analyses to be performed at the University of Windsor. The redox character of the collected samples was immediately determined (e.g. $HS^-$, Eh, $O_2$, pH) for each depth interval using the electrochemical methods described in Section 2.2 of this manuscript. All FFT samples were stored at 4 °C in the laboratory and archived for future molecular and mineralogical analysis at the University of Windsor.

### 3. Results and discussion

### 3.1. Biogeochemical alteration within the microcosms

Microcosms were inspected daily to document qualitative changes visible in the water column and the FFT material. By the end of 6 weeks, a clear zonation pattern had developed in all of the biotic microcosms, depicted by a persistent black sulfidic zone, visible just below the FFT–OSPW interface. This band occurred regardless of whether the microcosms were oxic or anoxic (Fig. 1). Such banding was never observed in any of the sterilized abiotic microcosms, suggesting that the development of the

sulfidic zone was likely driven by biological activity, most likely by SRP communities. Intriguingly, such a sulfidic zone was recently observed *in situ* in FFT tailing retention ponds, similarly at the FFT–OSPW interface, at water depths as great as ∼15 m (Ramos-Padrón et al., 2011; Chi Fru et al., 2013). The water column in the biotic microcosms, of both oxic and anoxic treatments became increasingly turbid through the course of the study relative to the abiotic microcosms, which remained minimally turbid throughout the study period. This turbidity has been ascribed to possible microbial growth in these systems (Chi Fru et al., 2013).

The oxic biotic microcosms exhibited a moderate increase in water-column pH over time, rising from ∼8.5 to 8.9, then decreasing to ∼7.7 in the FFT. A similar trend was observed for the oxic abiotic system, suggesting that abiotic processes most likely influenced changes in pH in these systems. In contrast, the anoxic microcosms showed no significant differences in the pH across the FFT–OSPW interface, regardless of whether the microcosm system was biotic or abiotic, ranging from pH ∼8.6 at week 6 to 8.9 after week 52, indicating that both compartments of the microcosm (water column and FFT) are in relative steady state with respect to H$^+$ activity. Both the oxic and anoxic pH data suggest little or no biotic influence on pH change in these systems. However, the consistent differences in pH pattern observed between the two atmosphere-related treatments suggest that O$_2$ likely exerts a critical influence on pH evolution at the FFT–OSPW interface. One of many possible reaction pathways would be the decomposition of organic matter in the systems, which may directly affect the HCO$_3^-$ concentration and lead to increased alkalinity (Tucker and D'Abramo, 2008). This is certainly possible in the context of the anoxic microcosms, since these types of reactions would influence the pH directly, as long as the reduced reaction products remain in a reduced state.

The water column in the oxic biotic microcosms exhibited an Eh of ∼400 mV throughout the experimental period, declining to a consistent value of ∼−200 mV within the FFT material, regardless of depth. In contrast, the Eh measured in the water column of the abiotic microcosms ranged from ∼250 to 400 mV, decreasing to ∼−100 mV within the FFT material. In comparison the anoxic biotic microcosms registered Eh values decreasing rapidly from ∼300 to −200 mV within the water column after week 1 and then stabilizing at ∼−200 mV in the FFT. Depth seemed to have little to no effect. The anoxic abiotic microcosms showed a similar pattern with respect to Eh values in the water column, but with a smaller dynamic range of 300–50 mV after week 1, ranging from ∼−50 to −100 mV in the FFT material. These Eh values generally affirm the highly reducing nature of the FFT, regardless of whether the water column is exposed to O$_2$ or not. These observations provide new information, suggesting that both biotic and abiotic processes may be playing significant roles in the distribution of total dissolved salts and ions in the FFT materials. However, the systems seem to be more strongly reducing in the presence of biotic activity, argued below to be tightly linked to sulfide production, which is especially true for the FFT material.

### 3.2. Oxygen profiles

Over the 52-week period, significant differences in O$_2$ consumption were observed between the abiotic and biotic microcosms exposed to oxic and anoxic conditions. Under anoxic conditions (Fig. 2), the similarities between the biotic and abiotic systems were immediately apparent. Under the anoxic environment dissolved O$_2$ was rapidly consumed. There were few or no observable differences between the O$_2$ concentrations measured in the water column and the FFT between the anoxic biotic and abiotic systems To determine the O$_2$ flux at the FFT–OSPW interface, changes in the O$_2$ concentrations over the first 6 weeks were measured and

compared to the net trends observed for the 52-week period. Here the total sediment O$_2$ demand (SOD) of the FFT is defined as representing the combined biological sediment O$_2$ demand (BSOD) plus the chemical sediment O$_2$ demand (CSOD). The CSOD in this case can be represented by the abiotic treatment (Fig. 2) (Slama, 2010). The average fluxes reported (a transport term defined by Fick's Law of diffusion) for the anoxic microcosms (Table 2), indicate that the flux of O$_2$ change was high ∼1.1 × 10$^3$ nmol cm$^{-2}$ s$^{-1}$ at the onset, whereas the net flux calculated over the entire 52 week period was ∼6.6 × 10$^2$ nmol cm$^{-2}$ s$^{-1}$. Oxygen in the overlying water was rapidly depleted in these anoxic microcosms (Fig. 2). Negligible O$_2$ concentrations (below 1 mg L$^{-1}$) were observed for the remainder of the experiment, regardless of whether the system was biotic or abiotic.

In the oxic microcosm treatments (Fig. 2), the concentrations of dissolved O$_2$ in the water column fluctuated. Initial concentrations were ∼6.8 mg L$^{-1}$ decreasing to 3.2 mg L$^{-1}$ at 6 weeks, and reaching equilibrium after 36 and 52 weeks with a final dissolved O$_2$ concentration of 5.4 mg L$^{-1}$ in the overlying water cap. Below the FFT/OSPW interface the O$_2$ concentration in these microcosm treatments decreased rapidly to <1 mg L$^{-1}$ similar to what was observed in the anoxic treatments. A comparison of these profiles (Fig. 2) contrasts the differences in O$_2$ concentrations in the oxic microcosm treatments determined over the 52 weeks (Table 2). It is important to note that the biotic microcosm contains a thriving bacterial community producing reduced reactants, that scavenge O$_2$, resulting in a decrease in concentration. This explains the increasing divergence in O$_2$ profiles between the biotic and abiotic systems over time. During the initial 52-week period, a net O$_2$ flux of 1.0 × 10$^{-1}$ nmol cm$^{-2}$ s$^{-1}$ was measured in the oxic biotic microcosms at the FFT–OSPW interface. However, the oxic abiotic microcosm showed the formation of a dissolved O$_2$ diffusion gradient below the FFT–OSPW interface. The dissolved O$_2$ concentrations 300 μm below the FFT–OSPW interface increase dramatically from 1.6, 3.8 and 5.1 mg L$^{-1}$ at weeks 24, 36 and 52 respectively. An O$_2$ flux of 1.6 × 10$^1$ nmol cm$^{-2}$ s$^{-1}$ was determined at the FFT–OSPW interface. The onset of this distinct dissolved O$_2$ gradient in the absence of any biological inputs can be considered to be representative of the FFT chemical sediment O$_2$ demand (CSOD). Its formation represents the depletion of residual reducing compounds present in the FFT mixture near the interface, and the establishment of O$_2$ equilibrium among the three reactive compartments (air, water, sediment). These results suggest that both biological (bacterial communities) and chemical factors (reduced compounds i.e. ammonia, sulfide, Fe(II) and CH$_4$) play a role in O$_2$ consumption within aerated systems at the FFT/OSPW interface (Maerki et al., 2009).

It should also be pointed out that these estimates of flux are much higher than rates of sediment O$_2$ demand measured in both eutrophic hypoxic sediments and 10–20 a-old wetlands, constructed with oil sands materials. Slama (2010) reported sediment O$_2$ demand (SOD) rates ranging from 2.6 × 10$^{-3}$ to 1.3 × 10$^{-2}$ nmol cm$^{-2}$ s$^{-1}$ in 8 wetlands containing FFT and OSPW. Gardner Costa (2010) estimated that approximately 80% of that SOD could be ascribed to chemical demand by reduced species. In contrast, the estimated O$_2$ flux to hypoxic sediments of organically enriched eutrophic lakes are slightly lower (1.5 × 10$^{-3}$ to 1.9 × 10$^{-3}$ nmol cm$^{-2}$ s$^{-1}$ in two European lakes (Matzinger et al., 2010); 4.0 × 10$^{-3}$ to 8.0 × 10$^{-3}$ nmol cm$^{-2}$ s$^{-1}$ in central Lake Erie of the Laurentian Great Lakes (Smith and Matisoff, 2008). Matzinger et al. (2010) attributed 40–80% of the flux to oxidation of reduced substances diffusing from the sediments, the majority of which were estimated to be emanating from sediments deposited within the last 10 a.

In ice-covered boreal systems O$_2$ in epibenthic layers of water becomes depleted by biological demand of which sediment is a dominant component. The reported O$_2$ fluxes of freshly produced FFT determined in these experiments are two orders of magnitude
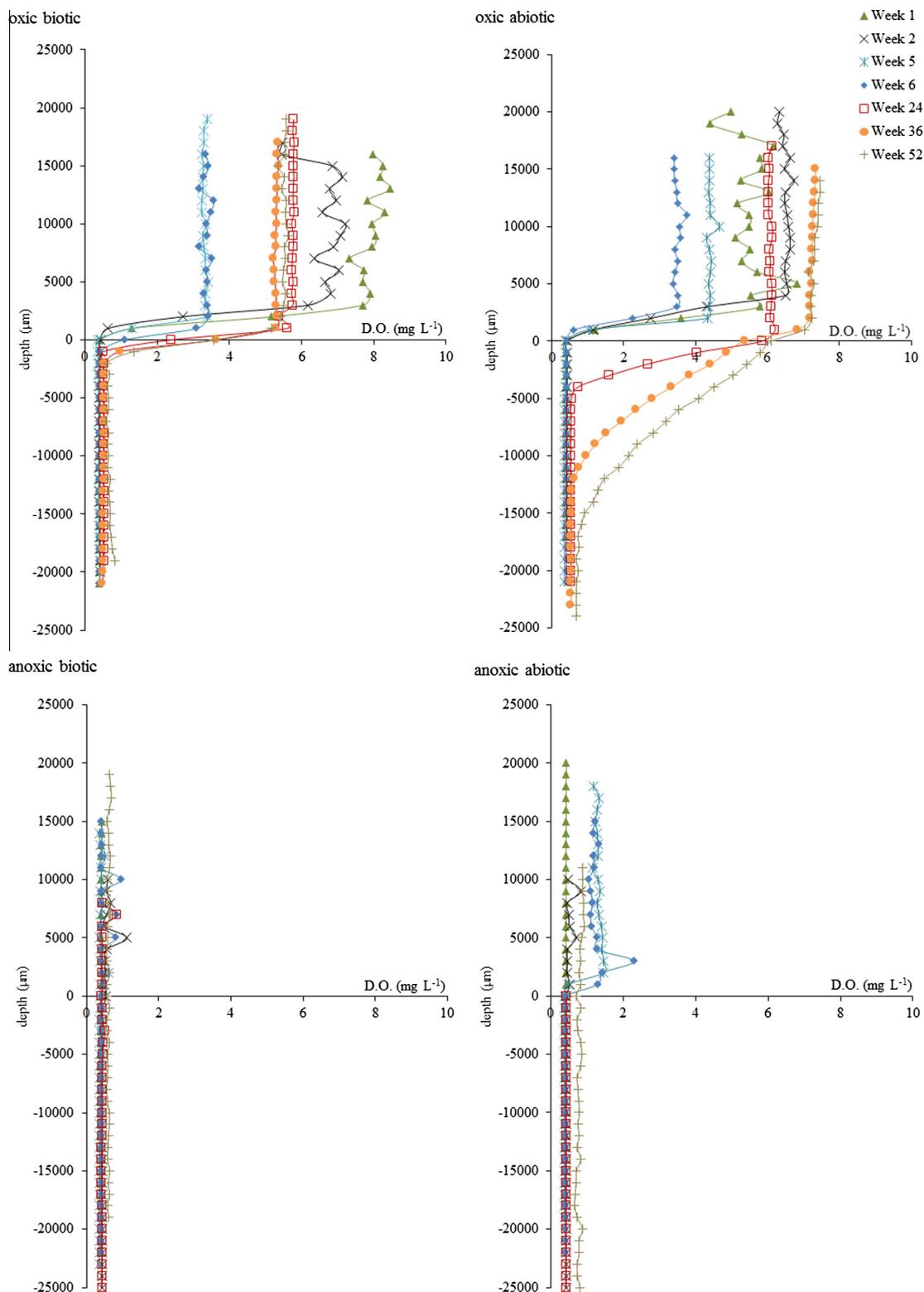
Fig. 2. Comparison of the oxygen profiles over a 52 week period. Oxygen profiles shown represent the oxic and anoxic treatments. Zero denotes the interface.

higher than those reported in natural systems and is a reflection of the strongly reducing nature of this material.

### 3.3. Hydrogen sulfide formation

For comparative purposes the concentrations of $HS^-$ were measured 1 cm below the FFT–OSPW interface. Hydrogen sulfide ($HS^-$) measured in both the oxic and anoxic abiotic microcosms (Fig. 3)

did not change over the 52-week period. In both cases, the $HS^-$ concentrations were below 10 $\mu$mol $L^{-1}$. By comparison, the oxic and anoxic biotic microcosms showed a significant increase in $HS^-$ production over the 52-week study period. The most marked changes occurred in the anoxic biotic treatment, where $HS^-$ concentrations increased from 41 $\mu$mol $L^{-1}$ at 1 week to 86 $\mu$mol $L^{-1}$ at 5 weeks. After the fifth week, the $HS^-$ concentrations gradually decreased within the FFT. At week 6 the $HS^-$ concentration

**Table 2**
Summary of short term and long-term oxygen and hydrogen sulfide fluxes at the FFT–OSPW interface.

| Species | Time (weeks) | FFT FLUXES ($nmol\ cm^{-2}\ s^{-1}$) | | |
|---|---|---|---|---|
| | | Oxic biotic | Anoxic biotic | Oxic abiotic (CSOD) |
| Dissolved oxygen | 6 | $1.0 \times 10^{-1}$ | $1.1 \times 10^3$ | – |
| (D.O.) | 52 | $\sim 1.0 \times 10^{-1}$ | $6.6 \times 10^2$ | $1.6 \times 10^1$ |
| Eutrophic Lake[a] (SOD) | Matzinger et al. (2010) | $1.5 \times 10^{-3}$ | | |
| Wetland FFT[a] (SOD) | Slama et al. (2010) | $2.6 \times 10^{-3}$ | | |
| Lake Erie[a] (SOD) | Smith and Matisoff (2008) | $4.0 \times 10^{-3}$ | | |
| Hydrogen sulfide (HS$^-$) | 6 | $2.9 \times 10^3$ | | $2.1 \times 10^3$ |
| | 52 | $8.2 \times 10^1$ | | $1.7 \times 10^2$ |

[a] Comparative SOD measurements from natural and constructed wetlands given as $O_2$ flux consumption.

decreased to 65 µmol L$^{-1}$ followed by a further decrease to 27 µmol L$^{-1}$ for weeks 24, 36 and 52 suggesting that equilibrium was reached between the processes dominating production and those that are consuming HS$^-$ in the FFT, after 24 weeks. Increases of HS$^-$ concentrations in the overlying water column in the anoxic microcosms correlated with peak HS$^-$ production after 5 and 6 weeks, reaching maximum concentrations of ~24 and 18 µmol L$^{-1}$, respectively, before decreasing to ~4 µmol L$^{-1}$ after 24 weeks. The results (Fig. 3) are supported by flux calculations (Table 2). Flux values for week 6 in the FFT were estimated to be $2.1 \times 10^3$ nmol cm$^{-2}$ s$^{-1}$, indicating significant HS$^-$ production. For the same time point, the flux in the water column was $5.8 \times 10^2$ nmol cm$^{-2}$ s$^{-1}$, suggesting that significant quantities of HS$^-$ diffused into the water column if the water column O$_2$ concentrations were below 1 mg L$^{-1}$. At 52 weeks, the flux in the FFT dropped to $1.7 \times 10^2$ nmol cm$^{-3}$ s$^{-1}$ (estimated from an average value calculated over the course of the entire year). This difference in flux may suggest a decrease in transport rather than reflecting a measure of consumption of HS$^-$ in the FFT. The profiles (Fig. 3) clearly show that a significant amount of HS$^-$ was still present in the FFT at the end of 52 weeks, and that the diffusion of HS$^-$ into the water column had decreased to $-1.0 \times 10^{-1}$ nmol cm$^{-2}$ s$^{-1}$ at the end of the experiment. These results suggest that little or no HS$^-$ was diffusing into the water cap after 52 weeks.

### 3.4. Implications of oxygen–hydrogen sulfide dynamics

Oxygen apparently played a minor role in net HS$^-$ generation in the FFT materials, likely due to the highly reducing nature of sulfide. This has implications for designing bioremediation systems and for evaluating the role sulfide production might have in the sustainability of EPLs over a long-term period.

The occurrence of an active sulfidic zone at the FFT–OSPW interface is certainly important. In a companion study, Chi Fru et al. (2013) estimated that it takes over a decade for this sulfidic zone to develop in *in situ* tailings ponds, linked to bacterial production of sulfide through SO$_4$-reduction. Because sulfide is such a strong reducer, the production of HS$^-$ in the FFT material likely contributes to the increase of reducing conditions in the biotic systems, as reported in Section 3.1; the detection of HS$^-$ is diagnostic of the anoxic conditions present.

Wang and Chapman (1999) reviewed the potentially important role of hydrogen sulfide on aquatic biota in a variety of aquatic systems. From a bioremediation perspective, HS$^-$ is of most concern in the water above the sediment of boreal systems both for its toxicity to biota and in its contribution to COD. Ice formation in winter both prevents re-aeration and reduces mixing of hypolimnetic water, leading to substantial depths of anoxia in Alberta lakes (Babin and Prepas, 1985). The additional chemical demand that could be imposed by oxidation of FFT-derived HS$^-$, at least in young systems, could ultimately determine whether or not fish would be able to persist in an EPL or whether infaunal and benthic invertebrates could survive the extended periods of hypoxia or anoxia that could develop in epibenthic waters during the winter.

The observations presented are especially pertinent to understanding of tailings reservoir function, as most studies of these systems to date have focused primarily on CH$_4$ production in tailings ponds (Holowenko et al., 2000; Fedorak et al., 2002). However, the profiles illustrate that biotically driven HS$^-$ production, most likely by S- and SO$_4$-reducing prokaryotes, may also be quite significant during the initial development of the storage facility and could apply to future end pit lake remediation strategy. The most noteworthy finding is the close degree to which the microcosms utilized in this study duplicate a pattern observed in the field (Ramos-Padrón et al., 2011). Consequently, the mechanisms deduced in this study likely explain that comparable scenario. As shown, these results describe an enrichment of sulfide in the biotic microcosm suggesting the HS$^-$ production gradient may continue deeper than the 2.5 cm depth from the FFT–OSPW interface and is consistent with *in situ* findings at Syncrude's WIP (Chi Fru et al., 2013). In that study, different scales are considered, where the sulfide zone culminates at 2.5 m below the FFT/OSPW interface of WIP. The presence of SO$_4$-rich zones has also been reported between 2 and 15 m below the FFT–OSPW interface near the center of Tailings Pond 6 (TP6), an active pond managed by Suncor Energy Inc. (Ramos-Padrón et al., 2011) and in Ponds STP and Pond 1A (not published). In light of this, the ratio of materials used in this experiment is comparable to volumes and processes monitored in WIP, where the depth of FFT is 35 m (T. Penner, Syncrude Canada, Ltd., pers. comm.). Furthermore, the microcosms developed microbial profiles whose patterns correlated with the depth and microbial diversity relationships reported *in situ*, in Syncrude's WIP FFT sample core materials (Chi Fru et al., 2013). This suggests that the microcosms both chemically and spatially are analogous although they represent a conservative static condition and may serve as important tools to model these systems for inferring *in situ* biogeochemical processes and evaluating the results of possible interventions required to manage future end pit lakes.

### 3.5. Metal sulfide formation

The XRD analysis (unpublished results) from the 1, 6 and 36-week period samples identified quartz, mica, feldspar minerals, accessory Fe sulfides, and amorphous Fe(III) oxides. The bulk mineralogy did not change during the course of the experiment, but an increase in Fe sulfide was detected at 36 weeks by XRD, and confirmed by quantitative particle analyses (Table 3). To compare background and post formation of *in situ* minerals (e.g. Fe sulfides) a combination of ESEM micrographs and particle analyses was performed on samples. ESEM micrographs of the starting material showed both amorphous Fe oxides and mature Fe sulfide grains (Fig. 4A). The pyrite grains observed in the starting FFT typically
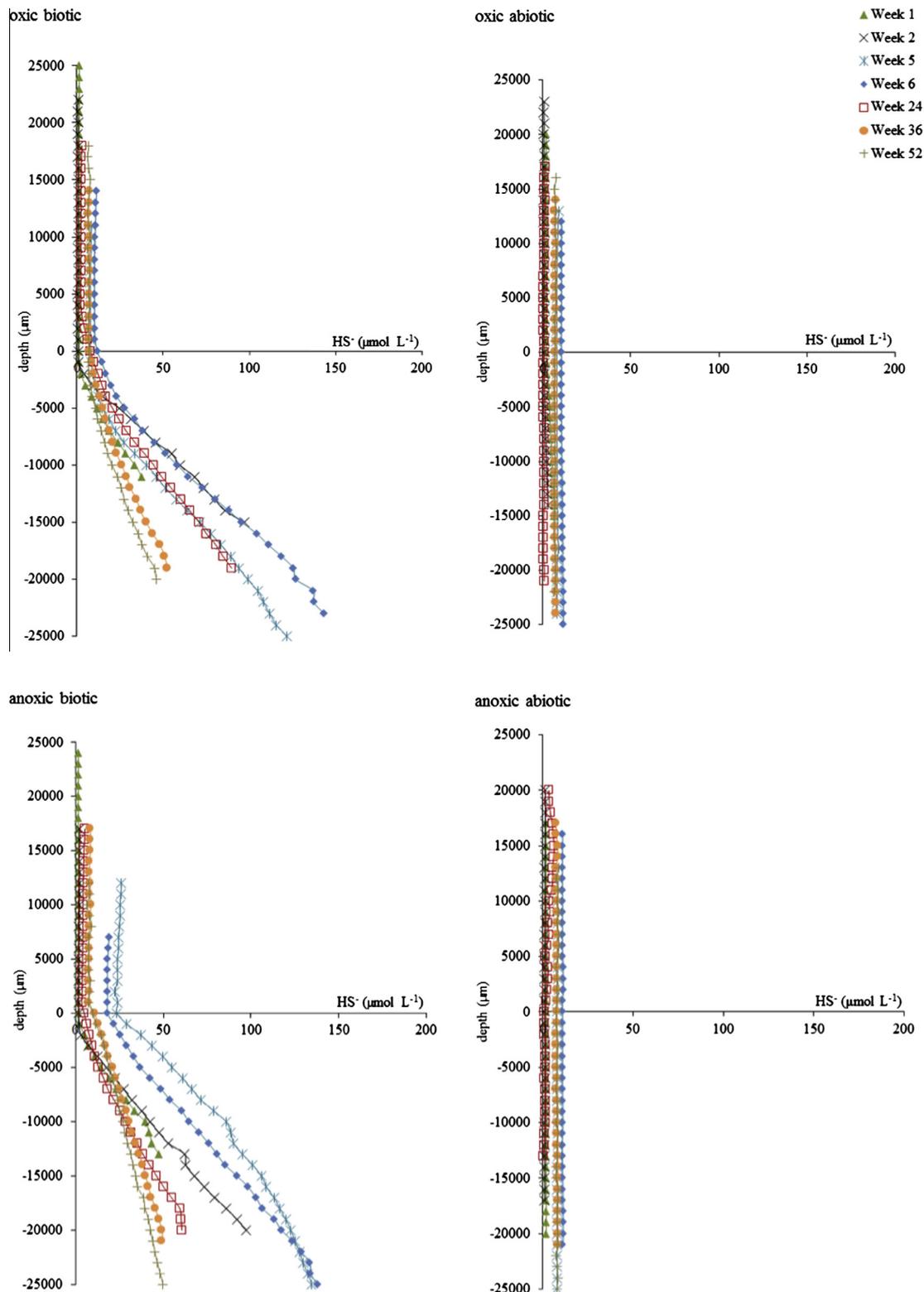
**Fig. 3.** Comparison of the hydrogen sulfide profiles over a 52 week period. Hydrogen sulfide profiles represent the oxic and anoxic treatments. After 24 weeks a decrease in the concentration of hydrogen sulfide is observed regardless of treatment.

consisted of large single euhedral grains ranging in size from 5 to 15 μm, in contrast to the aged samples, which illustrated noticeable change in size and shape. The 6 and 36-week FFT samples (Fig. 4B and C) showed more framboidal pyrite clusters typified by micro-morphological characteristics such as spherical aggregates of discrete equi-regular microcrystals (~0.2 μm). Analysis of the 6-week FFT samples by EDS (unpublished results) showed significant

differences in the sulfide chemical stoichiometry (typically 2:1 S:Fe observed in pyrite) from 1:1 to 1.5:1 S:Fe ratio. Analysis of the 36-week FFT samples revealed the presence of pyritic framboids with increased diameter ranging from 5 to 10 μm. The morphologies observed at this later stage suggest that a maturation effect continues to occur within the sulfide-rich band reported in the microcosms. Particle analysis of the 1 and 36-week FFT samples showed an

**Table 3**
The distribution of sulfide particles within the FFT treatments over 36 weeks.

| Sample | Treatment | Iron sulfides (%) | Average particles | Area sulfide (μm²) | Area clays (μm²) |
|---|---|---|---|---|---|
| Starting FFT | Anaerobic | −1.8 | >4000 | 2.519 | 1.806 |
| | Aerobic | −2.2 | | 2.841 | 1.734 |
| 36 | weeks | Anaerobic | | | 3.066 |
| | | −7.2 | | | |
| 1.861 FFT | Aerobic | −4.1 | | 2.764 | 1.29 |

increase in the relative proportion of Fe sulfide framboids over the duration of the experiment (Table 3). After 36 weeks there was an increase in the relative proportion of sulfide clusters from ∼2% in the starting FFT samples (both oxic and anoxic biotic treatments) compared to 4.1% for oxic and 7.2% for the anoxic abiotic treatments. These results suggest that the increase in Fe sulfide

production has a direct influence on the increasing pH over time in the FFT, as discussed in Sections 3.1 and 3.3, while Fe plays a role in HS⁻ removal, as is the case reported in other natural aquatic systems (Cornwell and Sampou, 1995; Chambers et al., 2000; Rickard and Morse, 2005). Pyrite formation has been reported at Eh values as low as −250 mV (Butler and Rickard, 2000) in the absence of $O_2$, similar to conditions reported in the microcosms in Sections 3.2 and 3.3.

### 3.6. Redox transition zone

The geochemical field scale profiles collected in September 2011 provide the first high-resolution *in situ* attempt combined with the microcosm investigations, to establish the clear existence of a redox transition zone within the WIP basin. Despite the overall sediment heterogeneity suggested by the deposition of materials, there exists a defined contrast between the physical materials deposited and the evolution of stratified geochemical and biotic
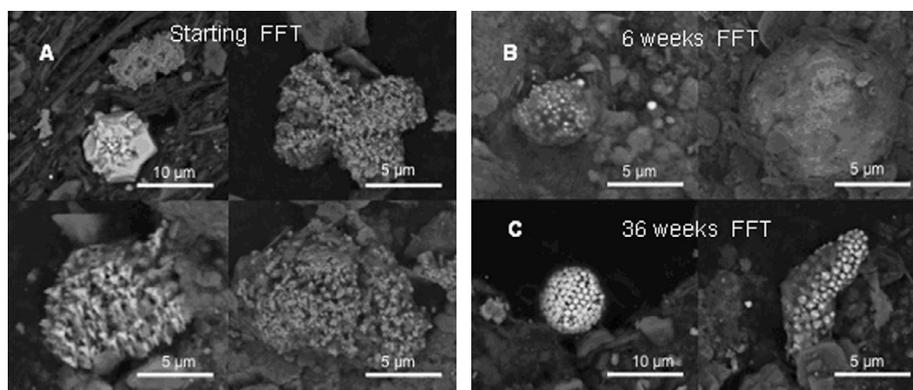


**Fig. 4.** Micrographs from FFT collected from the anoxic microcosms collected from a 1 cm depth below the interface over a 36 week period (A) Four SEMS micrographs show a variety sulfide and iron hydroxide minerals present from the original starting material (B) shows an example of newly formed iron sulfide particles collected after 6 weeks and coincides with the onset increased hydrogen sulfide concentration in the system. (C) shows progressive crystallization of iron sulfide framboids within the FFT after 36 weeks.
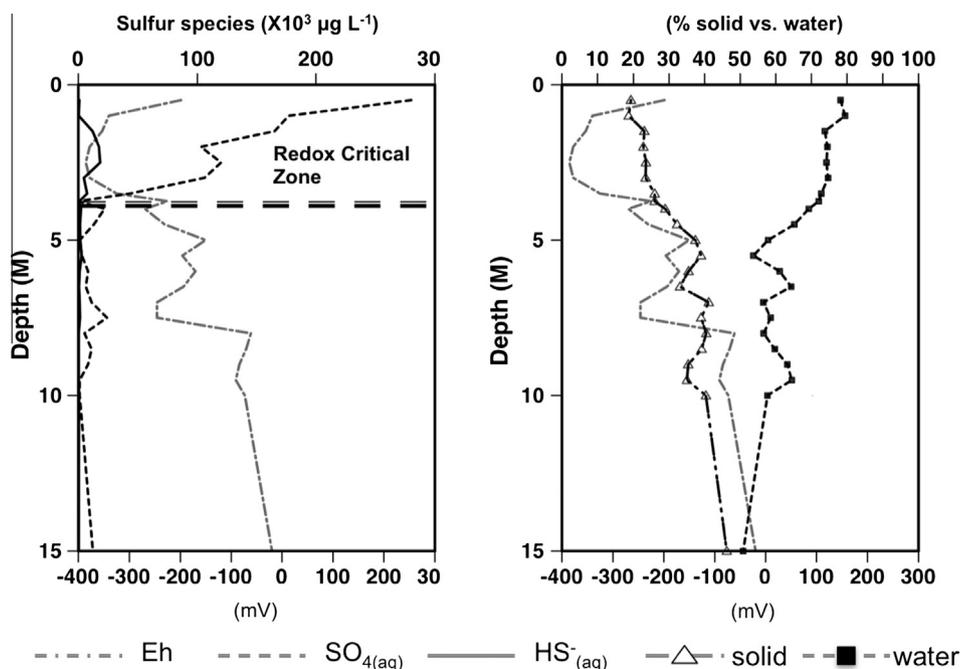


**Fig. 5.** Illustration of the distribution of sulfate and hydrogen sulfide as a function of Eh with depth within the sampled region of West In-Pit at this location. Along the depth axis zero denotes the approximate FFT/OSPW interface. Within the first 3 m redox transition zone is identified with a Eh minimum of -380mV. The open triangles and closed squares denote total solids and water content respectively.

signatures (Chi Fru et al., 2013). This assumption is supported by the demonstration of the development of a transition redox zone in the microcosms. This is strongly suggested to transcend a critical euxinic zone (sulfide-rich/$O_2$-poor), which is suppressed towards the bottom of the profile. This stratification seems to exhibit a niche-selective effect, enabling the development of a persistent bacterial assemblage, likely dominated by the $SO_4$-reducing pro-karyotes in the sulfidic zone (Penner and Foght, 2010; Chi Fru et al., 2013). The redox zonation of the FFT pond was suggested to play an important role for the subsequent emergence of the methanogenic Archaea in both the microcosms and WIP basin (Chi Fru et al., 2013). The geochemical profile (Eh, HS$^-$, $SO_4^{2-}$, % water, % solids profiles) in Fig. 5 collected from the top 15 m of the sediment layer suggests that a well-defined redox gradient develops within the first 5 m of the FFT–OSPW interface in the WIP basin. As already noted, a comparable small-scale version of this redox zonation was also observed in the microcosms. The field measurements revealed elevated concentrations of HS$^-$, ranging from 12 to 18 mg L$^{-1}$ between 1.5 to 2.5 m, respectively, within the FFT of the WIP basin, followed by a decrease to 7 mg L$^{-1}$ at 3.5 m. Measured $SO_4^{2-}$ concentrations decreased rapidly from 280 mg L$^{-1}$ recorded at the FFT–OSPW interface,(defined as zero m within the FFT zone), down to 120 mg L$^{-1}$ at 2.5 m, accounting for a decrease of more than 50%. Measured Eh values showed a distinct redox gradient developing between 0 m$_{(interface)}$ and 3 m, reaching −386 mV at 2.5 m, which coincides with the peak HS$^-$ production concentrations, measured at this location (Fig. 5). This suggests that biological activity is important in the redox development in this material as the HS$^-$ is assumed to be a product of biological activity. Although the measured Eh potentially reflects the sum of many redox reactions dominating a system it has been shown that a decrease in Eh from −200 to −300 mV can induce a 10-fold increase in $CH_4$ production and a 17-fold increase in its emission (LeMer and Roger, 2001). Another interesting trend which is very apparent is the process of densification subject to water loss which occurs between 5 to 10 m and subsequent depths. As a result of the reduction in physical pore space availability following densification, this likely controls nutrient transmission, and thus might partly explain the reduction in the abundance and diversity of microbial communities with depth (Chi Fru et al., 2013).

When the results and the interpretations of microcosm and field-wide studies are combined with the Eh measurements and the behavior of the S cycle (which is tightly linked to the selective spatial development of microbial community structures in the FFT material and ponds), it becomes evident that an active geochemical zone transcends into the first 3 m below the FFT–OSPW interface. The influence of this zone on the FFT–OSPW interface diminishes with depth, characterized by lower Eh potentials ($\sim$−75 mV) below 10 m and a suggested reduction in microbial diversity (Chi Fru et al., 2013).

## 4. Conclusions

The microsensors used in this study provide improved correlations for determining the biogeochemical environment at the FFT–OSPW interface, a critical zone that is suggested to be important for the understanding of how FFT materials deposited in open basins will change over longer-term scales (years to decades). Previous studies have highlighted the importance of $CH_4$ production from FFT but few have identified processes occurring across this redox boundary. This study shows that HS$^-$ production is very significant for the response of the short-term biophysico-chemical processes affecting FFT evolution over the long term. This appears to influence the development of viable microbial life, critical for the

transformation of the FFT basins into sustainable environments capable of supporting higher trophic level communities. The results in this paper show that the production of HS$^-$ may be a self-limiting process, the rates of which will begin to decrease after a period of time. The variables and rates measured for $O_2$ and HS$^-$ consumption and production will be useful for developing future models designed to understand EPL behavior. Predicting when HS$^-$ production will cease or how quickly the decrease will occur is not entirely possible from these results, as other variables influencing these systems require consideration. Although the microcosms have been shown to be near biological and chemical equivalents of the in situ field conditions, it must be recognized that there is considerable variability based on individual operator processing environments and deposition practice in the existing basins. The differing processing, generation and extraction techniques along with solvents used may influence the chemical development in these systems. Further investigations should focus on the spatial variability within the tailing ponds, confirming whether chemical and material variability will impact the development and depth of developing redox transition environments and active microbial contributions to water quality. It is clear that these experiments have provided a potentially useful diagnostic tool to monitor these systems, providing a ready resource that could be harnessed for the easy evaluation of biogeochemical concepts important for the safe disposal of FFT materials.

## References

Alberta Energy Government, 2013. <http://www.energy.gov.ab.ca/Oil/pdfs/FSRefining.pdf>.

Alberta Energy and Utilities Board, 2007. Alberta Ministry of Energy, Annual Report, 2006–2007.

Archer, D.E., Johnson, K., 2000. A model of the iron cycle in the ocean. Global Biogeochem. Cycles 14, 269–279.

Arega, F., Lee, J.H.W., 2005. Diffusional mass transfer at sediment–water interface of cylindrical sediment oxygen demand chamber. J. Environ. Eng. 131, 755–766.

Babin, J., Prepas, E.E., 1985. Modelling winter oxygen depletion rates in ice-covered temperate zone lakes in Canada. Can. J. Fish. Aquat. Sci. 42, 239–249.

Butler, I.B., Rickard, D., 2000. Framboidal pyrite formation via the oxidation of iron (II) monosulfide by hydrogen sulphide. Geochim. Cosmochim. Acta 64, 2665–2672.

Chalaturnyk, R.J., Scott, J.D., Özüm, B., 2002. Management of oil sands tailings. Petrol. Sci. Technol. 20, 1025–1046.

Chambers, R.M., Hollibaugh, J.T., Snively, C.S., Plant, J.N., 2000. Iron, sulfur, and carbon diagenesis in sediments of Tomales Bay, California. Estuar. Coasts 23, 1–9.

Chi Fru, E., Piccinelli, P., Fortin, D., 2012. Insights in to the global microbial community structure associated with iron oxyhydroxide minerals deposited in the aerobic biogeosphere. Geomicrobiol J. 29, 587–610.

Chi Fru, E., Chen, M., Walshe, G., Penner, T., Weisener, C.G., 2013. Bioreactor studies predict whole microbial population dynamics in oil sands tailings ponds. Appl. Microbiol. Biotechnol. 97, 3215–3224.

Church, M.J., Hutchins, D.A., Ducklow, H.W., 2000. Limitation of bacterial growth by dissolved organic matter and iron in the Southern Ocean. Appl. Environ. Microbiol. 66, 455–466.

Clemente, J.S., Fedorak, P.M., 2005. A review of the occurrence, analyses, toxicity, and biodegradation of naphthenic acids. Chemosphere 60, 585–600.

Cornwell, J.C., Sampou, P.A., 1995. Environmental controls on iron sulfide mineral formation in a coastal plain estuary. Environ. Sci. Technol. 612, 224–242.

Crowe, S.A., Roberts, J.A., Weisener, C.G., Fowle, D.A., 2007. Alteration of iron-rich lacustrine sediments by dissimilatory iron-reducing bacteria. Geobiology 5, 63–73.

Damgaard, L.R., Larsen, H., Revsbech, N.P., 1995. Microscale biosensors for environmental monitoring. Trancs-Trends Anal. Chem. 14, 300–303.

Elberling, B., Damgaard, L.B., 2001. Microscale measurements of oxygen diffusion and consumption in subaqueous sulfide tailings. Geochim. Cosmochim. Acta 65, 1897–1905.

Fedorak, P.M., Coy, D.L., Dudas, M.J., Simpson, M.J., Renneberg, A.J., MacKinnon, M.D., 2002. Microbially-mediated fugitive gas production from oil sands tailings and increased tailings densification rates. J. Environ. Eng. Sci. 2, 199–211.

Gardner Costa, J.C., 2010. Spatial and temporal variation in sediment-associated microbial respiration in oil sands mine-affected wetlands of north-eastern Alberta, Canada. MSc. Thesis, Univ. Windsor, ON Canada, pp. 54–87.

Gelda, R.K., Auer, M.T., Effler, S.W., 1995. Determination of sediment oxygen demand by direct measurement and by inference from reduced species accumulation. Mar. Freshwater Res. 46, 81–88.

Glud, R.N., 2008. Oxygen dynamics of marine sediments. Mar. Biol. Res. 4, 243–289.

Hofman, G., de Jong, S.A., Wagenvoort, E.J., Sandee, A.J.J., 1991. Apparent sediment diffusion coefficients for oxygen and oxygen consumption rates measured with microelectrodes and bell jars: applications to oxygen budgets in estuarine intertidal sediments (Oosterschelde, SW Netherlands). Mar. Ecol. Prog. Ser. 69, 261–272.

Holowenko, F.M., MacKinnon, M.D., Fedorak, P.M., 2000. Methanogens and sulfate-reducing bacteria in oil-sands fine tailings waste. Can. J. Microbiol. 46, 927–937.

Leahy, J.G., Colwell, R.R., 1990. Microbial degradation of hydrocarbons in the environment. Microbiol. Rev. 54, 305–315.

LeMer, J., Roger, P., 2001. Production, oxidation, emission and consumption of methane by soils: a review. Eur. J. Soil. Biol. 37, 25–50.

Maerki, M., Muller, B., Dinkel, C., Wehrli, B., 2009. Mineralization pathways in lake sediments with different oxygen and organic carbon supply. Limnol. Oceanogr. 54, 428–438.

Matzinger, A., Iler, B.M., Niederhauser, P., Schmid, M., Wu, A., 2010. Hypolimnetic oxygen consumption by sediment-based reduced substances in former eutrophic lakes. Limnol. Oceanogr. 55, 2073–2084.

Penner, T.J., Foght, J.M., 2010. Mature fine tailings from oil sands processing harbour diverse methanogenic communities. Can. J. Microbiol. 56, 459–470.

Ramos-Padrón, E., Bordenave, S., Lin, S., Bhaskar, I.M., Dong, X., Sensen, C.W., Fournier, J., Voordouw, G., Gieg, L.M., 2011. Carbon and sulfur cycling by microbial communities in a gypsum-treated oil sands tailings pond. Environ. Sci. Technol. 45, 439–446.

Revsbech, N.P., 1989. Diffusion characteristics of microbial communities determined by use of oxygen microsensors. J. Microbiol. Meth. 9, 111–122.

Revsbech, N.P., Nielsen, L.P., Ramsing, N.B., 1998. A novel microsensor for determination of apparent diffusivity in sediments. Limnol. Oceanogr. 43, 986–992.

Rickard, D., Morse, J.W., 2005. Acid volatile sulfide (AVS). Mar. Chem. 97, 141–197.

Rueter, P., Rabus, R., Wilkest, H., Aeckersberg, F., Rainey, F.A., Jannasch, H.W., Widdel, F., 1994. Anaerobic oxidation of hydrocarbons in crude oil by new types of sulphate-reducing bacteria. Nature 372, 455–458.

Salloum, M.J., Dudas, M.J., Fedorak, P.M., 2002. Microbial reduction of amended sulfate in anaerobic mature fine tailings from oil sand. Waste Manage. Res. 20, 162–171.

Schoonen, M.A.A., 2004. Mechanisms of sedimentary pyrite formation. Geol. Soc. Am. 379, 117–134.

Scott, A.C., MacKinnon, M.D., Fedorak, P.M., 2005. Naphthenic acids in Athabasca oil sands tailings waters are less biodegradable than commercial naphthenic acids. Environ. Sci. Technol. 39, 8388–8394.

Siddique, T., Fedorak, P.M., Foght, J.M., 2006. Biodegradation of short-chain $n$-alkanes in oil sands tailings under methanogenic conditions. Environ. Sci. Technol. 40, 5459–5464.

Siddique, T., Fedorak, P.M., MacKinnon, M.D., Foght, J.M., 2007. Metabolism of BTEX and naphtha compounds to methane in oil sands tailings. Environ. Sci. Technol. 41, 2350–2356.

Siddique, T., Penner, T., Semple, K., Foght, J.M., 2011. Anaerobic biodegradation of longer-chain $n$-alkanes coupled to methane production in oil sands tailings. Environ. Sci. Technol. 45, 5892–5899.

Slama, C., 2010. Sediment oxygen demand and sediment nutrient content of reclaimed wetlands in the oil sands region of northeastern Alberta. MSc. Thesis, Univ. Windsor, ON Canada, pp. 115–117.

Smith, D.A., Matisoff, G., 2008. Sediment oxygen demand in the central basin of Lake Erie. J. Great Lakes Res. 34, 731–744.

Sørensen, K., Řeháková, K., Zapomelová, E., Oren, A., 2009. Distribution of benthic phototrophs, sulfate reducers, and methanogens in two adjacent saltern evaporation ponds in Eilat, Israel. Aquat. Microb. Ecol. 56, 275–284.

Syncrude Canada Ltd., 1995. Syncrude Analytical. Methods Manual, 4th ed. Syncrude Research. Report 543.028S99R. Syncrude Canada Ltd., Edmonton, AB, Canada.

Tahey, T.M., Duineveld, G.C.A., Berghuis, E.M., Helder, W., 1994. Relation between sediment–water fluxes of oxygen and silicate and faunal abundance at continental shelf, slope and deep-water stations in the northwest Mediterranean. Mar. Ecol. Prog. Ser. 104, 119–130.

Tucker, C.S., D'Abramo, L.R., 2008. Managing high pH in freshwater ponds. Southern Reg Agriqua. Cen., 4604.

Wang, F.Y., Chapman, P.M., 1999. Biological implications of sulfide in sediment—a review focusing on sediment toxicity. Environ. Toxicol. Chem. 18, 2526–2532.

Wang, W., Reed, P., 1984. Additional fractionation of sediment oxygen demand. Environ. Int. 10, 51–53.

Weber, K.A., Achenbach, L.A., Coates, J.D., 2006. Microorganisms pumping iron: anaerobic microbial iron oxidation and reduction. Nat. Rev. Microbiol. 4, 752–764.

Weisener, C.G., Weber, P.A., 2010. Preferential oxidation of pyrite as a function of morphology and relict texture. N. Z. J. Geol. Geophys. 53, 22–33.

Williams, B., 2003. Heavy hydrocarbons playing key role in peak-oil debate, future energy supply. Oil Gas J. 101, 20–27.

Williford, K.H., Foriel, J., Ward, P.D., Steig, E.J., 2009. Major perturbation in sulfur cycling at the Triassic–Jurassic boundary. Geology 37, 835–838.